Innate immune signaling in hearts and buccal mucosa cells of patients with arrhythmogenic cardiomyopathy

Carlos Bueno-Beti, PhD,* Alessandro Tafuni, MD,† Stephen P. Chelko, PhD, FHRS,‡ Mary N. Sheppard, MD,* Ella Field, MSc,§ Jennifer Tollit, MSc,§ Imogen K. Heenan, BSc,§ Annabelle Barnes, BSc,§ Matthew R. Taylor, MD, PhD,|| Luisa Mestroni, MD,|| Juan Pablo Kaski, MD,§ Jeffrey E. Saffitz, MD, PhD, FHRS,¶[1] Angeliki Asimaki, PhD*[1]

*From the *Cardiovascular Academic and Clinical Academic Group and Cardiology Research Centre, Molecular and Clinical Sciences Research Group, St. George's, University of London, United Kingdom, †Department of Pathology, University of Parma, Parma, Italy, ‡Department of Biomedical Sciences, Florida State University College of Medicine, Tallahassee, Florida, §Centre for Inherited Cardiovascular Diseases, Great Ormond Street Hospital, London, United Kingdom, ||Cardiovascular Institute and Adult Medical Genetics Program, University of Colorado Anschutz Medical Campus, Aurora, Colorado, and ¶Department of Pathology, Beth Israel Deaconess Medical Center and Harvard Medical School, Boston, Massachusetts.*

BACKGROUND Nuclear factor κB (NF-κB) signaling in cardiac myocytes causes disease in a mouse model of arrhythmogenic cardiomyopathy (ACM) by mobilizing CCR2-expressing macrophages that promote myocardial injury and arrhythmias. Buccal mucosa cells exhibit pathologic features similar to those seen in cardiac myocytes in patients with ACM.

OBJECTIVES We sought to determine if persistent innate immune signaling via NF-κB occurs in cardiac myocytes in patients with ACM and if this is associated with myocardial infiltration of proinflammatory cells expressing CCR2. We also determined if buccal mucosa cells from young subjects with inherited disease alleles exhibit NF-κB signaling.

METHODS We analyzed myocardium from ACM patients who died suddenly or required cardiac transplantation. We also analyzed buccal mucosa cells from young subjects with inherited disease alleles. The presence of immunoreactive signal for RelA/p65 in nuclei of cardiac myocytes and buccal cells was used as a reliable indicator of active NF-κB signaling. We also counted myocardial CCR2-expressing cells.

RESULTS RelA/p65 signal was seen in numerous cardiac myocyte nuclei in 34 of 36 cases of ACM but not in 19 age-matched control individuals. Cells expressing CCR2 were increased in patient hearts in numbers directly correlated with the number of cardiac myocytes showing NF-κB signaling. NF-κB signaling was observed in buccal cells in young subjects with active disease.

CONCLUSIONS Patients with clinically active ACM exhibit persistent innate immune responses in cardiac myocytes and buccal mucosa cells, reflecting a local and systemic inflammatory process. Such individuals may benefit from anti-inflammatory therapy.

KEYWORDS Arrhythmogenic cardiomyopathy; Innate immune signaling; Nuclear factor κB; Proinflammatory macrophages; Buccal mucosa cells

(Heart Rhythm O^2 2023;4:650–659)

Introduction

Inflammation appears to contribute to the pathogenesis of arrhythmogenic cardiomyopathy (ACM), a familial nonischemic heart muscle disease characterized by arrhythmias and progressive myocardial injury, but its precise role is undefined. Inflammatory infiltrates occur typically in the hearts of ACM patients, and their abundance has been correlated with hot phases of the disease associated with more frequent arrhythmias and accelerated myocardial injury.[1,2] However, the exact identity of immune cells within the hearts of ACM patients and mechanisms driving their infiltration into the myocardium remain unknown. We have previously reported that inhibition of nuclear factor κB (NF-κB) signaling rescues the disease phenotype in a mouse model of ACM involving homozygous knock-in of a variant in the gene encoding the desmosomal protein, desmoglein-2 (*Dsg2$^{mut/mut}$* mice).[3] In subsequent studies, we observed that

[1]Drs Saffitz and Asimaki contributed equally to this work. **Address reprint requests and correspondence:** Dr Angeliki Asimaki, Cardiovascular Academic and Clinical Academic Group and Cardiology Research Centre Molecular and Clinical Sciences Research Group, St. George's, University of London, Cranmer Terrace, London, United Kingdom SW17 0RE. E-mail address: aasimaki@sgul.ac.uk.

2666-5018/

https://doi.org/10.1016/j.hroo.2023.09.006

KEY FINDINGS

- The nuclear factor κB (NF-κB) signaling cascade, a major driver of the innate immune response, is activated in cardiac myocytes in patients with arrhythmogenic cardiomyopathy (ACM).
- NF-κB signaling in cardiac myocytes in ACM is associated with myocardial accumulation of cells expressing CCR2, which are known to mediate tissue injury and fibrosis.
- Given the involvement of NF-κB signaling pathways in ACM, anti-inflammatory therapy may be of benefit for those with clinically active disease.
- As NF-κB signaling is also activated in buccal mucosa cells at the time of cardiac disease onset or exacerbation, evaluation of buccal mucosal cells could be useful to monitor ACM activity and response to therapy.

NF-κB signaling in cardiac myocytes is sufficient to drive the disease phenotype in *Dsg2*$^{mut/mut}$ mice.[4] Using a genetic approach to selectively prevent activation of NF-κB signaling in cardiac myocytes alone virtually eliminated myocardial degeneration and its replacement by fibrosis, preserved contractile function, and greatly reduced arrhythmias.[4] We also observed a 5-fold increase in the number of monocytes/macrophages expressing CCR2 (CCR2+ cells) in the hearts of *Dsg2*$^{mut/mut}$ mice but no increase after blocking NF-κB signaling in cardiac myocytes.[4] CCR2 is a G protein–coupled receptor for a monocyte chemoattractant family that includes monocyte chemoattractant protein-1 (aka CCL2). CCR2+ macrophages have been implicated in adverse cardiac remodeling[5,6] and fibrosis,[7] and monocyte chemoattractant protein-1 expression is increased in hearts of *Dsg2*$^{mut/mut}$ mice and in ACM patient induced pluripotent stem cell-cardiac myocytes.[3,8] Furthermore, genetic deletion of *Ccr2* greatly reduces myocardial injury and arrhythmias in *Dsg2*$^{mut/mut}$ mice.[4] Taken together, these results indicate that NF-κB signaling in cardiac myocytes drives myocardial injury, contractile dysfunction, and arrhythmias, at least in part, by mobilizing injurious proinflammatory CCR2+ macrophages to the heart.

In light of new mechanistic insights gained through studies of mouse models of ACM, we sought to determine if NF-κB signaling is activated in cardiac myocytes in ACM patients and, if so, whether this is associated with accumulation of myocardial CCR2+ cells. Furthermore, based on previous studies showing that buccal mucosa cells from ACM patients exhibit characteristic changes in the distribution of desmosomal and gap junction proteins similar to those seen in ACM patient hearts,[9,10] we also sought to determine if NF-κB signaling is activated in buccal mucosa cells obtained from young individuals with inherited ACM alleles. Evidence of active NF-κB signaling was indicated by the presence of immunoreactive signal for RelA/p65, the heterodimeric binding partner of NF-κB, in nuclei of cardiac myocytes or buccal mucosa cells, whereas cytoplasmic signal alone meant NF-κB was not activated. Using this approach, we observed active NF-κB signaling in cardiac myocytes in hearts from ACM patients associated with a marked increase in CCR2+ cells. There was a close correlation between the number of myocardial nuclei showing positive RelA/p65 signal and the number of myocardial CCR2+ cells in each case. We also observed NF-κB signaling in buccal mucosa cells from young ACM gene carriers, which correlated with disease activity and/or the first onset of clinical manifestations of disease.

Methods

Ethical approval

This study was approved by the UK National Health Service Research Ethics Committee (hearts: 17/LO/0747, buccal smears: 17/LO/0840). Informed consent was provided by next of kin at the time of autopsy and by parents/guardians of children whose buccal cells were sampled.

Myocardial samples

Myocardial samples were analyzed from 36 ACM patients and 19 control subjects. Clinical, diagnostic, and genetic information is shown in Table 1. Samples were obtained at autopsy from 29 ACM patients who had died suddenly, from explanted hearts of 6 ACM patients at heart transplantation, and from an endomyocardial biopsy performed in 1 ACM patient during internal defibrillator placement. Control myocardial samples came from age-matched subjects who died from noncardiac causes and had no cardiovascular disease at autopsy (Table 1).

Buccal mucosa samples

Buccal mucosa cells were obtained from 28 young individuals (5–17 years of age) using a soft cytological brush as previously reported.[9,10] Clinical, diagnostic, and genetic information is shown in Table 2. These subjects either were ACM probands or had a family history of ACM (21 were carriers of ACM disease alleles) and were being followed clinically at Great Ormond Street Hospital. Buccal cells were obtained from 12 preclinical carriers of variants who had never shown clinical disease, 3 at the clinic visit following the first clinical manifestation of disease, 9 with a quiescent clinical picture at the time cells were obtained (termed "stable" in Table 2), and 4 sampled during or shortly after clinical exacerbation of disease (termed "hot phase" in Table 2). Buccal smears from 22 children (1–17 years of age) without clinical signs or family history of cardiomyopathy were used as negative control individuals.

Immunoperoxidase staining of myocardial samples

Formalin-fixed, paraffin-embedded ventricular myocardium from all ACM patients and control individuals was analyzed by immunoperoxidase staining using a primary antibody

Table 1 Clinical, genetic, and immunohistochemical data of myocardial samples

Study	Clinical/PM data: Cause of death	Age at death (y)	Sex	Genetic data	RelA/p65 signal	Mean number of positive nuclei per mm^2 section area
CTR						
CTR1	Murder	37	M	NA	Cytoplasmic	2.1
CTR2	Drowning	29	M	NA	Cytoplasmic	0
CTR3	Electrocution	24	M	NA	Cytoplasmic	1.1
CTR4	Drug overdose	20	F	NA	Cytoplasmic	1.1
CTR5	Neck compression	40	M	NA	Cytoplasmic	0
CTR6	Murder	34	M	NA	Cytoplasmic	1.1
CTR7	Drug overdose	30	F	NA	Cytoplasmic	1.1
CTR8	Suicide	21	M	NA	Cytoplasmic	0
CTR9	Drug overdose	21	M	NA	Cytoplasmic	0
CTR10	Drug overdose	21	M	NA	Cytoplasmic	0
CTR11	Drug overdose	35	M	NA	Cytoplasmic	1.1
CTR12	Drug overdose	28	M	NA	Cytoplasmic	0
CTR13	Drug overdose	26	M	NA	Cytoplasmic	1.1
CTR14	Suicide	30	M	NA	Cytoplasmic	0
CTR15	Head injury	32	M	NA	Cytoplasmic	1.1
CTR16	Drowning	19	M	NA	Cytoplasmic	0
CTR17	Car accident	49	M	NA	Cytoplasmic	0
CTR18	Pulmonary embolism	29	M	NA	Cytoplasmic	1.1
CTR19	Car accident	23	F	NA	Cytoplasmic	0
ACM						
ACM1	SCD; PM Dx: RV-dom ACM	37	M	*PKP2*; c.2198_2202 delACACC	Nuclear	69.5
ACM2	SCD; PM Dx: RV-dom ACM	21	M	*PKP2*; Gln133X	Nuclear	49.5
ACM3	SCD; PM Dx: RV-dom ACM	20	M	*PKP2*; c.253_256delGAGT	Nuclear	58.9
ACM4	SCD; PM Dx: RV-dom ACM	34	M	*PKP2*; Ser688Pro	Nuclear	54.7
ACM5	SCD; PM Dx: biventricular ACM	20	M	*PKP2*; 1216delG	Cytoplasmic	2.1
ACM6	SCD; PM Dx: biventricular ACM	21	M	*PKP2*; 2013delC	Nuclear	58.9
ACM7	SCD; PM Dx: biventricular ACM	26	F	*DSP*; c.4395T>G	Nuclear	56.8
ACM8	SCD; PM Dx: biventricular ACM	28	M	*DSP*; c.5269C>T	Nuclear	65.2
ACM9	Biopsy at ICD implantation; Dx: biventricular ACM	Currently 35	F	*DSP*; c.3045del	Cytoplasmic	1.1
ACM10	SCD; PM Dx: LV-dom ACM	36	F	*DSP*; R1113X	Nuclear	57.9
ACM11	SCD; PM Dx: LV-dom ACM	28	F	*DSP*; c.5318del	Nuclear	56.8
ACM12	SCD; PM Dx: biventricular ACM	29	M	*Dsg2*; 2036delG	Nuclear	56.8
ACM13	SCD; PM Dx: biventricular ACM	18	M	*Dsc2*; G371fsX378	Nuclear	43.1
ACM14	SCD; PM Dx: biventricular ACM	34	M	*Dsc2;* E896fsX900	Nuclear	51.6
ACM15	SCD; antemortem Dx: Naxos disease	21	M	*JUP*; 2157del2, homozygous	Nuclear	58.9
ACM16	SCD; PM Dx: biventricular ACM	21	M	*PKP2*; R735Q & *DSP*; R270X	Nuclear	66.3
ACM17	SCD; PM Dx: biventricular ACM	32	M	*Dsg2;* M1I & *Dsg2;* I333T	Nuclear	74.7
ACM18	SCD; PM Dx: biventricular ACM	20	M	*TMEM43*; c.1073C>T	Nuclear	22.1
ACM19	SCD; PM Dx: biventricular ACM	45	M	*TMEM43*; c.1073C>T	Nuclear	36.8
ACM20	SCD; PM Dx: RV-dom ACM	20	M	*FLNC*; c.7552-1 G>A	Nuclear	43.1
ACM21	SCD; PM Dx: RV-dom ACM	36	M	*FLNC*; c.6779A>G	Nuclear	50.5
ACM22	Transplant; Dx: biventricular ACM + HF	NA	NA	*PLN*; R14del	Nuclear	46.3
ACM23	Transplant; Dx: biventricular ACM + HF	NA	NA	*PLN*; R14del	Nuclear	48.4
ACM24	Transplant; Dx: biventricular ACM + HF	NA	NA	*PLN*; R14del	Nuclear	45.2
ACM25	Transplant; Dx: biventricular ACM + HF	NA	NA	*PLN*; R14del	Nuclear	37.9
ACM26	Transplant; Dx: biventricular ACM + HF	NA	NA	*PLN*; R14del	Nuclear	54.7
ACM27	SCD; antemortem Dx: ACM	37	M	NA	Nuclear	42.1
ACM28	SCD; PM Dx: biventricular ACM	23	F	NA	Nuclear	64.2
ACM29	SCD; PM Dx: biventricular ACM	37	M	NA	Nuclear	43.1
ACM30	SCD; PM Dx: RV-dom ACM	41	F	NA	Nuclear	46.3
ACM31	SCD; PM Dx: RV-dom ACM	20	M	NA	Nuclear	70.5
ACM32	SCD; antemortem Dx: ACM	40	M	NA	Nuclear	53.7
ACM33	SCD; PM Dx: biventricular ACM	24	M	NA	Nuclear	60
ACM34	SCD; PM Dx: biventricular ACM	43	M	NA	Nuclear	64.2
ACM35	SCD; PM Dx: biventricular ACM	33	M	NA	Nuclear	54.7
ACM36	Transplant; Dx: biventricular ACM + HF	Currently 47	M	No result on panel testing	Nuclear	45.2

ACM = arrhythmogenic cardiomyopathy; CTR = control; Dx = diagnosis; F = female; HF = heart failure; ICD = implantable cardioverter-defibrillator; LV-dom = left ventricular dominant; M = male; NA = not available; PM = postmortem; RV-dom = right ventricular dominant; SCD = sudden cardiac death.

Table 2 Clinical, genetic, and immunocytochemical data for buccal smear samples

Study	Age (y)	Sex	Genetic data	Clinical status at time of sampling	Disease status	RelA/p65 signal distribution
pACM1	13	F	*PKP2*; c.148_151delACAG	Normal cardiac investigations to date	Preclinical	Cytoplasmic
pACM2	12	F	*DSP*; c.7756C>T	Normal cardiac investigations to date	Preclinical	Cytoplasmic
pACM3	11	M	*DSP*; Arg84X	Borderline left axis deviation; normal cardiac investigations	Preclinical	Cytoplasmic
pACM4	16	M	*PKP2*; Thr50Ser*61	Normal cardiac investigations to date	Preclinical	Cytoplasmic
pACM5	16	F	*PKP2*; Thr50Ser*61	Normal cardiac investigations to date	Preclinical	Cytoplasmic
pACM6	18	F	*PKP2*; Thr50Ser*61	Normal cardiac investigations to date	Preclinical	Cytoplasmic
pACM7	11	M	*DSP*; c.1755_1756insA	Normal cardiac investigations to date	Preclinical	Cytoplasmic
pACM8	8	M	*DSP*; c.1755_1756insA	Normal cardiac investigations to date	Preclinical	Cytoplasmic
pACM9	15	M	*PKP2*; c.337-2A>T	Normal cardiac investigations to date	Preclinical	Cytoplasmic
pACM10	12	F	*DSP*; Trp180Ter	Sibling of pACM22; small voltages in ECG leads; normal cardiac investigations	Preclinical	Cytoplasmic
pACM11	15	F	*DSP*; p.Arg2160Ter	Normal cardiac investigations to date	Preclinical	Cytoplasmic
pACM12	5	F	*DSP*; Gln 2692* homozygous	Normal cardiac investigations to date; extracardiac features include palmoplantar keratoderma, nail dystrophy, sparse hair and keratosis follicularis	Preclinical	Cytoplasmic
pACM13	16	F	*DSP*; Arg2160X	Intraventricular conduction delay in V4 and early repolarization inferiorly and in V4–V6 compared with previous clinical investigations	Initial disease onset	Nuclear
pACM14	17	M	*DSP*; Arg2160X	Early repolarization inferiorly and in V5, V6; SAECG showed late potentials in 1 vector; moderate RV dilatation on cMRI compared with previous investigations	Initial disease onset	Nuclear
pACM15	17	F	No pathogenic variants detected on gene panel	Evaluated after developing exertional syncope and light headedness associated with hyperventilation; T-wave inversions in V1–V3; positive SAECG in 2 vectors; frequent ectopy	Initial disease onset	Nuclear
pACM16	12	F	*DSP*; Leu622Pro	Previous diagnosis of ACM and erythrokeratoderma; frequent ectopy; biventricular dilatation; mildly impaired systolic function	Stable	Cytoplasmic

(*Continued*)

Table 2 (*Continued*)

Study	Age (y)	Sex	Genetic data	Clinical status at time of sampling	Disease status	RelA/p65 signal distribution
pACM17	14	M	Not tested	Previous diagnosis of ACM; NSVT episodes on Holter monitoring.	Stable	Cytoplasmic
pACM18	15	M	No pathogenic variants detected on gene panel	Previous diagnosis of ACM; ventricular ectopy on exertion; focal LGE on cMRI involving inferoseptal LV on cMRI; symptomatic narrow complex tachycardia on loop recorder	Stable	Cytoplasmic
pACM19	17	M	No pathogenic variants detected on gene panel	Previous diagnosis of ACM; ventricular ectopy; exertional VT; borderline LV dilatation; impaired systolic function	Stable	Cytoplasmic
pACM20	17	M	No pathogenic variants detected on gene panel	Previous diagnosis of ACM; NSVT; abnormal repolarization on resting ECG	Stable	Cytoplasmic
pACM21	17	F	No pathogenic variants detected on gene panel	Previous diagnosis of ACM; positive SAECG in 3 vectors; SVT on Holter monitoring; LGE in mid-wall basal anterior septum on cMRI	Stable	Cytoplasmic
pACM22	17	M	*DSP*; Trp180Ter	Sibling of pACM10; previous diagnosis of ACM; right axis deviation; subendocardial LGE on cMRI involving LV free wall; normal LV volume with preserved systolic function	Stable	Cytoplasmic
pACM23	11	M	*DSP*; c.7576delAAGA and *DSP*; c.6577G>A	Previous diagnosis of ACM; frequent ventricular ectopy; NSVT; previous sustained VT and mildly impaired LV and RV global systolic function	Stable	Cytoplasmic
pACM24	16	M	*PKP2*; Thr50Ser*61	Previous diagnosis of ACM; RV internal dimensions at upper limit of normal; SAECG positive in 2 vectors	Stable	Cytoplasmic
pACM25	10	F	*PKP2*; Lys859Asn, homozygous	Severe biventricular dilatation; impaired systolic function; frequent ectopy; VT; ICD in situ; on active cardiac transplant list	Hot phase	Nuclear
pACM26	17	F	Results pending	Previous diagnosis of ACM with multifocal arrhythmia ablation in 2016; at time of buccal sampling, patient exhibited palpitations, dizziness and atrial tachycardia	Hot phase	Nuclear

Table 2 (*Continued*)

Study	Age (y)	Sex	Genetic data	Clinical status at time of sampling	Disease status	RelA/p65 signal distribution
pACM27	9	F	*PKP2*; c.2489+1 G>A	Previous diagnosis of ACM; at time of buccal sampling, patient was being seen in clinic after a recent episode of palpitations, pallor and perioral cyanosis; ventricular triplets on ambulatory ECG monitoring	Hot phase	Nuclear
pACM28	8	F	*SCN5A*; Arg222Gln	Previous diagnosis of ACM with LV dilatation and impaired global systolic function; at time of buccal sampling, patient showed >1000 PVCs/hour on ambulatory ECG monitor prompting ICD implantation	Hot phase	Nuclear

F = female; ECG = electrocardiogram; cMRI = cardiac magnetic resonance imaging; ECG = electrocardiography; ICD = implantable cardioverter-defibrillator; LGE = late gadolinium enhancement; LV = left ventricular; M = male; NSVT = nonsustained ventricular tachycardia; pACM = pediatric ACM; PVC = premature ventricular complex; RV = right ventricular; SAECG = signal-averaged electrocardiogram; SVT = supraventricular tachycardia; VT = ventricular tachycardia.

against RelA/p65. Wherever possible, sections from the left ventricle, right ventricle, and interventricular septum of the same heart were immunostained. Otherwise, sections of left ventricle were analyzed. Sections (5 μm thick) were deparaffinized, dehydrated, rehydrated, and exposed to 3% hydrogen peroxide solution for 10 minutes to block endogenous peroxidase activity. Sections were then incubated first with blocking solution for 1 hour and then with a rabbit polyclonal anti-RelA antibody (LS-B653; LSBiosciences, Shirley, MA) overnight at 4°C. The following day, sections were incubated with donkey secondary antibody conjugated to horseradish peroxidase enzyme (1 hour). Peroxidase-conjugated antibodies were detected by the DAB substrate kit. Heart tissue was counterstained with Mayer's hematoxylin. Bright-field images were obtained from 5 randomly selected fields per section using a Nikon eclipse 80i microscope and recorded with Nikon DS-Fi1 camera (Nikon, Tokyo, Japan). All images were assessed by 2 independent observers (C.B.-B. and A.A.) who were blinded to all specific clinical information. The number of myocyte nuclei showing strong brown signal was counted in 5 randomly selected fields and expressed as the mean number of positive nuclei per mm^2 section area. Each staining batch included at least 2 ACM patient samples and 2 control samples.

Immunofluorescence staining for CCR2

When sufficient tissue was available, additional myocardial sections were analyzed by immunofluorescence staining using a primary antibody against CCR2. Sections (5 μm thick) were deparaffinized, dehydrated, rehydrated, and boiled in citrate buffer (pH = 6.0) for 11 minutes. They were then first incubated with blocking solution for 1 hour and then with a mouse monoclonal anti-human CCR2 antibody (MAB150-SP; R&D Systems, Minneapolis, MN) overnight at 4°C. The following day, sections were incubated with anti-mouse IgG Cy3-labeled secondary antibody and mounted with ProLong Gold (Thermo Fisher Scientific, Waltham, MA). Images from 5 randomly selected fields per section were recorded using a Nikon A1R confocal microscope. The number of cells showing strong immunofluorescent signal was counted in 5 randomly selected fields and expressed as number of cells per mm^2 section area.

Immunocytochemistry of buccal cells

Buccal cells were smeared on glass slides and fixed by M-FIX spray (Merck Millipore, Billerica, MA). They were then incubated first with blocking solution for 1 hour and then with a rabbit polyclonal anti-RelA antibody (8242; Cell Signaling Technology, Danvers, MA) overnight at 4°C. The following day, samples were incubated with anti-rabbit IgG Cy3-labeled secondary antibody, counterstained with DAPI and mounted with ProLong Gold. Images from 5 randomly selected fields per section were recorded using a Nikon A1R confocal microscope. Each staining batch included a least 1 ACM sample and 2 control samples.

Statistical analysis

GraphPad Prism software (version 9.2.0; GraphPad Software, San Diego, CA) was used for the statistical analysis of the CCR2+ cell data. The normal distribution of the data was assessed by Kolmogorov-Smirnov test. Normally distributed data were analyzed for differences by 1-way analysis of variance and the Newman-Keuls posttest for multiple

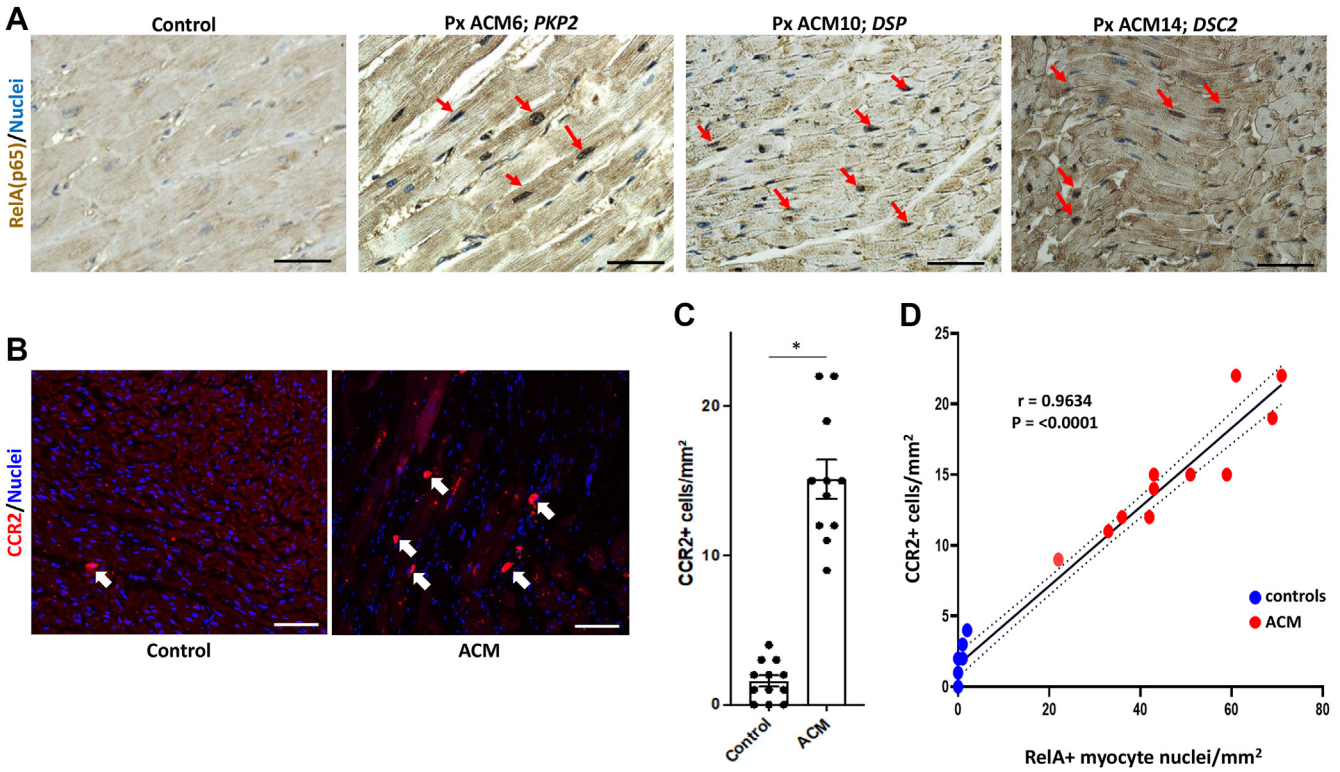

Figure 1 Expression of RelA/CCR2 in patient myocardial samples. **A:** Representative RelA/p65 immunoperoxidase staining in myocardial samples from control individuals and arrhythmogenic cardiomyopathy (ACM) patients. Brown nuclear signal (red arrows) in cardiac myocytes occurred only in ACM samples (×40). Scale bars = 50 μm. **B:** Representative CCR2 immunofluorescent staining in myocardial samples from control individuals and ACM patients. White arrows show CCR2-immunoreactive signal in small interstitial cells (×20). Scale bars = 100 μm. **C:** The number of CCR2+ cells/mm^2 section area in control and ACM patient heart samples; mean ± SEM; *$P < .0001$ vs control individuals; 1-way analysis of variance with Tukey multiple comparison test. **D:** The number of CCR2+ cells vs RelA/p65+ myocyte nuclei per mm^2 section area in 11 ACM and 12 control individuals; *$P < .0001$ vs control individuals determined by Pearson's r correlation with 95% confidence intervals (dashed lines).

comparisons. Pearson's correlation coefficient (r) was used to assess the linear correlation between CCR2+ cells and RelA+ myocyte nuclei. Data are presented as the mean ± SEM. A P value <.05 was deemed significant.

Data availability

Additional data and immunostaining images will be provided by the corresponding author upon request.

Results

NF-κB signaling is activated in cardiac myocytes in ACM patients

Strong immunoperoxidase signal for RelA/p65 was seen in cardiac myocyte nuclei in 34 of 36 ACM patient samples but in none of the 19 control samples. Representative examples are shown in Figure 1A. ACM cases showing positive signal had a mean of 50.33 ± 15.8 positive myocyte nuclei per mm^2 section area, whereas control cases showed few if any positive nuclei (0.57 ± 0.64 per mm^2 section area; $P < .0001$) (Table 1). In cases in which sections from the left ventricle, right ventricle, and interventricular septum of the same heart were immunostained, no apparent regional differences were seen in the proportion of myocyte nuclei showing RelA/p65 signal regardless of the presence of typical histological abnormalities. Nuclear signal indicating activation of NF-κB occurred in ACM patients with variants in all 5 desmosomal genes as well as variants in *FLNC*, *TMEM43*, and *PLN* (Table 1). The 2 ACM cases with no RelA/p65 nuclear signal (ACM5 and ACM9 in Table 1) had variants in *PKP2* and *DSP*, respectively. It is not clear why these cases showed no evidence of activation of NF-κB in cardiac myocytes. Nine ACM cases came from individuals who died suddenly out of hospital in whom the diagnosis of ACM was made on the basis of autopsy findings. No genetic screening information was available for these cases, but they all showed distinctive anatomic features of ACM at autopsy and clear evidence of active NF-κB signaling in cardiac myocytes.

CCR2+ cells are increased in hearts of ACM patients

In all control and ACM cases in which sufficient tissue was available, the number of CCR2+ cells per unit section area was determined by counting cells showing strong immunoreactive signal for CCR2 (Figure 1B). ACM hearts contained 15.2 ± 4.1 CCR2+ cells per mm^2 section area compared with 1.7 ± 1.4 cells per mm^2 section area for control hearts ($P < .0001$) (Figure 1C). Cells showing positive signal were small and round and were located between cardiac myocytes, consistent with their being macrophages (Figure 1B).

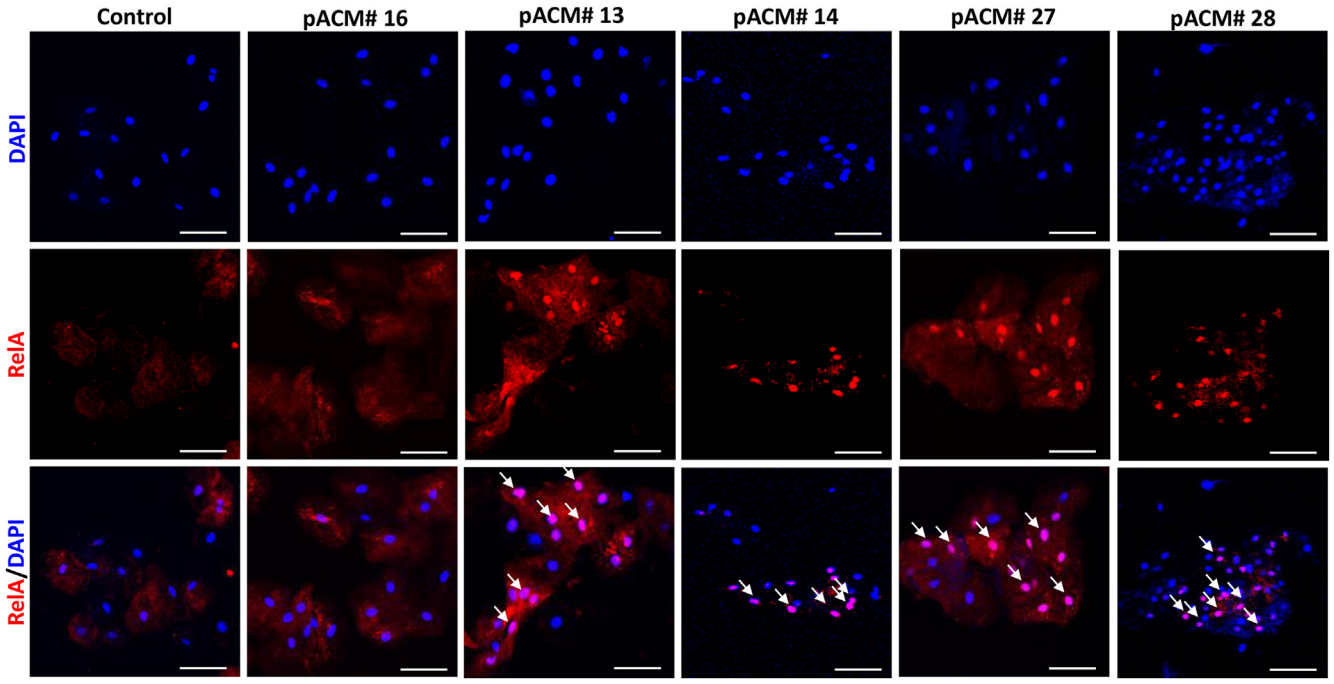

Figure 2 Expression of RelA in patient buccal smears. Representative RelA/p65 immunofluorescent staining in buccal cells from a control subject and pediatric arrhythmogenic cardiomyopathy (ACM) patients including those with stable disease (pediatric ACM [pACM]# 16), at initial manifestation of disease (pACM# 13, pACM# 14) or during a hot phase of disease deterioration (pACM# 27, pACM# 28). Nuclear RelA/p65 signal (white arrows) occurred only in patients undergoing phenoconversion or hot phases. Cell nuclei (blue) were counterstained with DAPI (×40). Scale bars = 50 μm.

Our studies in *Dsg2*$^{mut/mut}$ mice showed that NF-κB signaling in cardiac myocytes was responsible for mobilizing CCR2+ cells to the heart, where they promoted myocardial injury and arrhythmias.[4] Accordingly, we compared the average number of cardiac myocyte nuclei showing immunoreactive signal for RelA/p65 and the average number of CCR2+ cells per mm^2 section area in each case. As shown in Figure 1D, there was a close correlation, consistent with the causal mechanistic relationship observed in *Dsg2*$^{mut/mut}$ mice.[4]

NF-κB signaling is activated in buccal mucosa cells in young ACM patients with active disease

Buccal cells from the 12 ACM gene carriers with no clinical evidence of disease and the 9 patients with established but stable, quiescent disease showed no nuclear signal for RelA/p65, nor was nuclear signal seen in buccal cells from any of the 22 control individuals ($P < .0001$). By contrast, all 7 ACM gene carriers sampled either when clinical disease was first manifest or during hot phases showed strong RelA/p65 signal in buccal cell nuclei. Representative images are shown in Figure 2. Two subjects who showed nuclear RelA/p65 signal during a hot phase exhibited no nuclear signal in previous buccal smears analyzed 7 and 12 months before the onset of the hot phase (pACM27 and pACM26, respectively) (Table 2). Another patient with stable quiescent disease (pACM13) showed loss of nuclear signal in buccal cells analyzed 20 months after initial disease manifestation, whereas the nuclear signal persisted in a repeat sample in a patient (pACM28) who had presented with a dramatic arrhythmia burden 2 months earlier, despite reduced arrhythmias after amiodarone therapy.

Discussion

We have previously reported that inhibition of NF-κB signaling rescues the disease phenotype in *Dsg2*$^{mut/mut}$ mice.[3] NF-κB signaling is also activated in induced pluripotent stem cell–cardiac myocytes derived from patients with disease-causing variants in *PKP2* and *DSG2*.[3,8] These cells produce and secrete large amounts of proinflammatory mediators under basal conditions in vitro without prior stimulation or provocation. Taken together, these results suggest that innate immune signaling in ACM is a persistent, cell-autonomous inflammatory process that fails to resolve.

Here, we provide evidence that NF-κB is activated in cardiac myocytes in ACM patients. We observed nuclear signal for RelA/p65 in cardiac myocytes, a reliable indicator of active NF-κB signaling, in hearts of ACM patients who died suddenly and in others with advanced disease requiring cardiac transplantation. These observations suggest that as in *Dsg2*$^{mut/mut}$ mice,[4] ACM patients with clinically active disease exhibit a persistent innate immune response that does not resolve. We also provide new evidence linking NF-κB signaling in cardiac myocytes with accumulation of CCR2+ cells in the hearts of ACM patients. These results suggest that persistent innate immune signaling in cardiac myocytes may be a major driver of disease in AMC patients, as it is in *Dsg2*$^{mut/mut}$ mice. If so,

then ACM patients with clinically active disease might benefit from anti-inflammatory therapy that blocks NF-κB signaling, as we have demonstrated in *Dsg2*$^{mut/mut}$ mice.[3] In addition, imaging methods to quantify myocardial CCR2+ cells might also identify patients at greatest risk of adverse events in ACM.

We also show here that NF-κB signaling is activated in buccal mucosa cells of young ACM gene carriers at the time of disease onset or exacerbation. This observation extends previous findings indicating that ACM patients have a cutaneous phenotype, albeit subclinical, in which nonkeratinized buccal epithelial cells exhibit features similar to those seen in cardiac myocytes in ACM.[9,10] It remains unexplained how ACM alleles persistently activate innate immune signaling pathways, but our findings suggest that inflammation in ACM extends beyond the heart, consistent with previous studies showing elevated circulating levels of proinflammatory cytokines in ACM patients.[11]

We acknowledge several limitations in this work. ACM is a relatively uncommon disease and it is difficult to study the hearts of patients with documented disease. Nearly all available tissue specimens used in this study were formalin-fixed and paraffin-embedded, which limited the range of possible studies. It would have been desirable to independently validate activation of NF-κB signaling in cardiac myocytes by documenting expression of NF-κB-related target genes or proteins, but as a practical matter, such studies were not possible mainly because of limited tissue availability and lack of non–formalin-fixed tissue. Nevertheless, the presence of nuclear signal for RelA/p65 in cardiac myocytes in 34 of 36 ACM hearts and its absence in 19 control hearts is compelling evidence of innate immune signaling within cardiac myocytes, which we have shown in experimental models is necessary and sufficient to drive myocardial injury and arrhythmias in ACM.[4] Furthermore, active innate immune signaling was seen in cardiac myocytes in patients with variants in all 5 desmosomal genes and other genes linked to ACM including *FLNC*, *TMEM43*, and *PLN*. Thus, persistent immune signaling in cardiac myocytes appears to be a characteristic features across a broad clinical and genetic spectrum of ACM patients. We acknowledge that the presence of cells expressing CCR2 in hearts of ACM patients does not prove they caused myocardial injury. In addition, because of limited tissue availability, we did not independently document that cells expressing CCR2 were macrophages. CCR2 is most highly expressed in proinflammatory monocytes/macrophages in the heart,[12] which we have shown are increased 5-fold in the hearts of *Dsg2* $^{mut/mut}$ ACM mice.[4] CCR2 can also be expressed in endothelial cells or fibroblasts but generally in much lower amounts than in myeloid cells,[12] and we did not observe significant CCR2 expression in endothelial cells or fibroblasts in our ACM mouse studies.[4] Thus, we are confident that the small, round interstitial cells showing bright immunofluorescent signal for CCR2 in the hearts of ACM patients were myeloid cells and not endothelial cells or fibroblasts, which have much different morphology. Furthermore, this is the first report to our knowledge documenting marked infiltration of CCR2+ cells in ACM patient hearts, and these cells have been directly implicated in mediating tissue injury and fibrosis.[4–7,12] We also recognize that a relatively small number of young ACM gene carriers was studied but opportunities to analyze this patient population is also limited. Moreover, the consistent presence of active NF-κB signaling in buccal cells in young disease gene carriers at the time of disease onset or exacerbation is a remarkable new finding with considerable clinical implications. Taken together, our observations directly implicate persistent immune signaling in the pathogenesis of ACM and provide a compelling rationale for future clinical trials of anti-inflammatory therapy to block NF-κB. Finally, it is worth emphasizing that these studies would never have been possible by analyzing endocardial biopsies from young ACM gene carriers, whereas obtaining repeat buccal mucosa samples even from young children is safe, painless and well tolerated by patients and their families. In view of the ease of obtaining and analyzing buccal smears, screening these cells for evidence of immune activation may help identify patients who would benefit from anti-inflammatory therapies.

Acknowledgments

The authors thank the patients and their families who participated in this study.

Funding Sources: This work was supported by grants from the British Heart Foundation (PG/18/27/33616; Carlos Bueno-Beti, Angeliki Asimaki), the RosetreesFoundation (M689; Angeliki Asimaki), and the U.S. National Institutes of Health (R01-HL148348 [Jeffrey E. Safitz, Stephen P. Chelko], R01HL164634 and R01HL147064 [Luisa Mestroni, Matthew R. Taylor]). Juan Pablo Kaski was supported by a Medical Research Council–National Institute for Health Research Clinical Academic Research Partnership award. Ella Field, Annabelle Barnes, and Juan Pablo Kaski were supported by Max's Foundation and Great Ormond Street Hospital Children's Charity. Jennifer Tollit was jointly funded by Health Education England and the National Institute for Health Research. Imogen K. Heenan was supported by the Arrhythmogenic Cardiomyopathy Trust. This work was partly funded by the National Institute for Health Research Great Ormond Street Hospital Biomedical Research Centre.

Disclosures: Jeffrey E. Saffitz has received research support from Pfizer and Implicit Bioscience. Stephen P. Chelko has received research support from Pfizer and Rejuvenate Bio. All other authors have no conflicts of interest to disclose.

Authorship: All authors attest they meet the current ICMJE criteria for authorship.

Patient Consent: Informed consent was provided by next of kin at the time of autopsy and by parents/guardians of children whose buccal cells were sampled.

Ethics Statement: This study was approved by the UK National Health Service Research Ethics Committee (hearts: 17/LO/0747, buccal smears: 17/LO/0840).

References

1. Corrado D, Basso C, Thiene G, et al. Spectrum of clinicopathologic manifestations of arrhythmogenic right ventricular cardiomyopathy/dysplasia: a multicenter study. J Am Coll Cardiol 1997;30:1512–1520.
2. Lopez-Ayala JM, Pastor-Quirante F, Gonzalez-Carrillo J, et al. Genetics of myocarditis in arrhythmogenic right ventricular dysplasia. Heart Rhythm 2015; 12:766–773.

3. Chelko SP, Asimaki A, Lowenthal J, et al. Therapeutic modulation of the immune response in arrhythmogenic cardiomyopathy. Circulation 2019; 140:1491–1505.
4. Chelko SP, Penna V, Engel M, et al. Mechanisms of innate immune injury in arrhythmogenic cardiomyopathy. bioRxiv doi:10.1101/2023.07.12.548682.
5. Patel B, Bansai SS, Ismahil MA, et al. CCR2^{+} Monocyte-derived infiltrating macrophages are required for adverse cardiac remodeling during pressure overload. J Am Coll Cardiol Basic Trans Science 2018;3:230–244.
6. Bajpai G, Bredemeyer A, Li W, et al. Tissue resident CCR2- and CCR2+ cardiac macrophages differentially orchestrate monocyte recruitment and fate specification following myocardial Injury. Circ Res 2019;124:263–278.
7. Braga TT, Correa-Costa M, Silva RC, et al. CCR2 contributes to the recruitment of monocytes and leads to kidney inflammation and fibrosis development. Inflammopharmacol 2018;26:403–411.
8. Hawthorne RN, Blazeski A, Lowenthal J, et al. Altered electrical, biomolecular, and immunologic phenotypes in a novel patient-derived stem cell model of desmoglein-2 mutant ARVC. J Clin Med 2021;10:3061.
9. Asimaki A, Protonotarios A, James CA, et al. Characterizing the molecular pathology of arrhythmogenic cardiomyopathy in patient buccal mucosa cells. Circ Arrhythm Electrophysiol 2016;9:e003688.
10. Bueno Beti C, Field E, Tsatsopoulou A, et al. Analysis of buccal mucosa as a prognostic tool in children with arrhythmogenic cardiomyopathy. Prog Pediatr Cardiol 2022;64:101458.
11. Asimaki A, Tandri H, Duffy ER, et al. Altered desmosomal proteins in granulomatous myocarditis and potential pathogenic links to arrhythmogenic right ventricular cardiomyopathy. Circ Arrhythm Electrophysiol 2011;4:743–752.
12. Yerra VG, Advani A. Role of CCR2-positive macrophages in pathological ventricular remodeling. Biomedicines 2022;10:661.